Molecular dynamics simulation of four-α-helix bundles that bind the anesthetic halothane

Lowri A. Davies[a], Qingfeng Zhong[a], Michael L. Klein[a,*], Daphna Scharf[b]

[a] *Center for Molecular Modeling, Department of Chemistry, University of Pennsylvania, Philadelphia, PA 19104-6323, USA*
[b] *Department of Anesthesia, University of Pennsylvania Medical Center, Philadelphia, PA 19104-4283, USA*

Received 23 February 2000; revised 16 June 2000

Edited by Maurice Montal

Abstract The mutation of a single leucine residue (L38) to methionine (M) is known experimentally to significantly increase the affinity of the synthetic four-α-helix bundle $(A\alpha_2)_2$ for the anesthetic halothane. We present a molecular dynamics study of the mutant $(A\alpha_2–L38M)_2$ peptide, which consists of a dimer of 62-residue U-shaped di-α-helical monomers assembled in an anti topology. A comparison between the simulation results and those obtained for the native $(A\alpha_2)_2$ peptide indicates that the overall secondary structure of the bundle is not affected by the mutation, but that the side chains within the monomers are better packed in the mutant structure. Unlike the native peptide, binding of a single halothane molecule to the hydrophobic core of $(A\alpha_2–L38M)_2$ deforms the helical nature of one monomer in a region close to the mutation site. Increased exposure of the cysteine side chain to the hydrophobic core in the mutant structure leads to the enhancement of the attractive interaction between halothane and this specific residue. Since the mutated residues are located outside the hydrophobic core the observed increased affinity for halothane appears to be an indirect effect of the mutation.

Key words: Halothane; Four-α-helix bundle $(A\alpha_2)_2$; Anesthetic-protein interaction

1. Introduction

An understanding of the structural features of binding sites for inhaled anesthetics on proteins has been extensively pursued by many different approaches. Inhaled anesthetics alter the function of numerous membrane ion channels [1,2] and ion transport proteins [3], however, the mechanism involved remains poorly understood. Do these anesthetics bind to specific sites in membrane proteins or is there an indirect effect due to the perturbation of the lipid membrane by the anesthetics? Current opinion favors the former explanation [4–6] and several experimental studies have illustrated the existence of discrete sites for anesthetics in membrane and in water soluble proteins [4]. The complexity of membrane protein and current experimental limitations hinder direct probing of inhaled anesthetics binding sites in protein. Experimental advances with de novo synthetic peptides [7–11], which model native proteins, suggest an alternative approach. More specifically, the introduction of a simple cavity [12–14] into a designed four-α-helix structure by replacing six core leucines with alanines increases the affinity of the peptide for the anesthetic halothane ($CF_3CBrClH$) by a factor of 4.4 [11]. In addition, when L at position 38 is replaced with M (see Fig. 1), experimental studies show that this mutated peptide $(A\alpha_2–L38M)_2$ has a higher affinity (by a factor of 3.4) for halothane compared with the native $(A\alpha_2)_2$ one [15]. Such design-dependent phenomena indicate the importance of studying synthetic peptides whose structural features can be carefully controlled and monitored. Another advantage of model systems with known amino acid sequences and secondary structure, is that they can also be examined using computer simulation techniques such as molecular dynamics (MD). By using this approach detailed information can be obtained with respect to the peptide–anesthetic interactions, in particular the existence of attractive interactions between halothane and specific amino acid side chains are isolated.

Several plausible explanations have been advanced for the increased halothane affinity of $(A\alpha_2–L38M)_2$ [15]: the optimized size of the cavity inside the four-α-helix scaffold due to the smaller size of the M side chain; the direct interaction of halothane with the M side chain due to a favorable electrostatic contribution; and the increased access to the hydrophobic core for the anesthetic molecules due to the higher mobility of the M side chain. However, conclusive experimental evidence in support of any of these proposals is limited. Therefore, the aim of this theoretical study is to provide insight into the structure and changes that may occur in the bundle $(A\alpha_2–L38M)_2$ as a result of the single mutation and halothane binding.

2. Simulation system and methodology

The four-α-helix peptide studied consists of two 62-residue U-shaped di-α-helical monomers, denoted as $A\alpha_2$, each composed of two 27-residue α-helical stretches joined by an 8-residue flexible G linker. The sequence is based on prior designs [16–18] and is known experimentally to be water soluble and to bind halothane with high affinity in the hydrophobic core, as probed by quenching of the fluorescence emission of the two W residues. The two monomers can associate in either an anti [17,19] or syn [20,21] topology. Both experimental [11] and MD simulation [22] results indicate that the anti topology of the native $(A\alpha_2)_2$ peptide is more energetically favorable. Thus we only perform simulations for the mutant peptide $(A\alpha_2–L38M)_2$ in the anti topology. Residues on different monomers are distinguished by the label B.

The initial coordinates for the mutant peptide were obtained from a fully equilibrated configuration of the native peptide $(A\alpha_2)_2$ in aqueous solution taken from our work [22] after 1 ns of constant pressure and temperature (NPT) molecular dynamics at $P = 1$ atm and $T = 298$ K, which we summarize herein. Insight II software (Molecular Simulation Inc., San Diego, CA 92121, USA, Version 97.2) was utilized to construct the $A\alpha_2$ di-α-helical monomer. Two $A\alpha_2$ monomers were

*Corresponding author. Fax: (1)-215-898 8296.
E-mail: klein@lrsm.upenn.edu

0014-5793/00/$20.00
PII: S0014-5793(00)01792-0

positioned in anti topology at a distance, which allowed for residual dimer interaction. The resulting structure was placed to a pre-equilibrated water solvent environment ($T = 298$ K and $P = 1$ atm) and any overlapping water molecules were removed. The simulation system thus consisted of the peptide in a box with dimensions of $56 \times 56 \times 75$ Å^3 containing $\sim$6600 water molecules, with the long axis of the protein placed parallel to the long axis of the box.

Initial minimization of the system was performed using the steepest descent algorithm in CHARMM [23], which ensures that none of the protein atoms has any unfavorable contacts with one another or with any of the water molecules. Equilibration of the system consisted of 200 ps constant volume and temperature (NVT) MD at $T = 298$ K, followed by 150 ps of constant NPT MD at $P = 1$ atm and $T = 298$ K. An NPT MD trajectory was then generated for 1 ns at $P = 1$ atm and $T = 298$ K. The multiple time-step MD simulation algorithm of the PINY-MD computational package was implemented [24,25], which incorporates features such as periodic boundary conditions, Nosé–Hoover chain thermostats and PME-Ewald to evaluate the long-range interactions [26]. The interaction energy of the system consists of both intra- and inter-molecular components; bond stretching, bond–angle bending and torsions were all explicitly accounted for. The inter-molecular interactions were repulsive at short separations and attractive at intermediate separations; electrostatic interactions are also included in the total potential energy function. The AMBER-95 parameter set [27–29] was used to describe the protein interactions and the TIP3P model [30] for water was employed. All the O–H bonds in water and the bonds formed with hydrogen in the protein were constrained to their equilibrium value, enabling a time-step of 6 fs to be used.

To construct the mutant bundle $(A\alpha_2\text{–}L38M)_2$, the two L residues at position 38 and 38B were mutated to M in the equilibrated structure of $(A\alpha_2)$, using Insight II software. The resulting structure was placed back to the water solvent environment and any overlapping water molecules were removed. The same equilibration procedure as described for $A\alpha_2$ was used to equilibrate the mutant bundle $(A\alpha_2\text{–}L38M)_2$. Energy conservation combined with diminishing RMS deviations for structural properties (e.g. inertia tensor, lengths of the helices, secondary structure ψ and ϕ angles) were used to determine equilibrium.

Following 1 ns of dynamics two cavities exist between the four-α-helices in the mutant $(A\alpha_2\text{–}L38M)_2$ structure, each is large enough to accommodate a single halothane molecule. A single halothane molecule was placed in one of the hydrophobic cavities and an additional set of MD simulations were performed for the mutant bundle with a halothane molecule. This choice of initial condition was directed by the experimental results [11,15]. We note that in the anti topology the two hydrophobic cavities are identical due to symmetry.

Halothane was initially constructed using Insight II and the interaction parameters of Scharf and Laasonen [31] were used; the cross terms were evaluated with the Lorentz–Bertholot mixing rules. As for the system without halothane, minimization procedure was performed, followed by 200 ps of constant NVT MD at $T = 298$ K, and 150 ps of constant NPT simulation at $P = 1$ atm and $T = 298$ K, before a 1 ns MD trajectory was generated. On the timescale of the simulation the halothane molecule can rotate and translate in the cavity.

3. Results and discussion

During 1 ns of simulation the peptide scaffold of $(A\alpha_2\text{–}L38M)_2$ remains stable. Each of the four α-helices retains a high degree of α-helicity, and they twist to form a right-handed coiled-coil bundle. All the hydrophilic residues occupy positions, which maximize their contact with water, while the hydrophobic residues remain inside the core of the bundle. At equilibrium no water molecules are found within this hydrophobic region. Other structural features such as the components of the inertia tensor, and the lengths of the helices, only show small fluctuations during the simulation. These properties of the mutant $(A\alpha_2\text{–}L38M)_2$ mimic those observed for the simulation of the native $(A\alpha_2)_2$ peptide [22].

One significant difference between the overall structures of the mutant and native peptides is the increased interaction

(a)

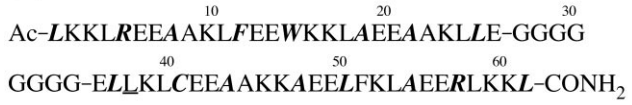

(b)

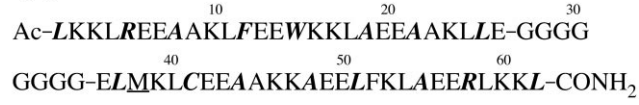

Fig. 1. Sequences of the di-α-helical monomers (a) native and (b) mutant. The hydrophobic residues, which occupy the heptad a and d positions inside the core of the bundle are shown in bold italics and the mutated residue is underlined. In the experimental design of the halothane cavity, six Leu residues were replaced by Ala in positions 9, 19, 23, 44, 45, and 48 [11] to produce the $A\alpha_2$.

between the two α-helices on the same monomer in the mutant $(A\alpha_2\text{–}L38M)_2$ protein. This results in an improved packing of hydrophilic side chains between the two α-helices connected by the G linker. Consequently the hydrophobic residues between the two monomers are more exposed to the solvent than in the native $(A\alpha_2)_2$ structure (see Fig. 2). This altered arrangement of side chains with respect to the solvent in the mutant $(A\alpha_2\text{–}L38M)_2$ peptide can be understood in terms of the variation of interactions between amino acid side chains in the vicinity of the mutation site. For example, the interaction between E27 and M38 (and between E27B and M38B) during the simulation has a significantly attractive van der Waals component whereas there is no corresponding attraction between E27 and L38 in the native $(A\alpha_2)_2$ peptide. Substitution of a single L with M in each monomer thus enhances the attractive interactions between side chains on the same $A\alpha_2$–L38M monomer, which leads to their closer proximity and hence improved packing.

The relative position of the mutated residue M38 with respect to that of L38 in the native peptide is not significantly different, both residues occupy a region that is not completely within the hydrophobic core of the four-α-helix structure (see Fig. 3). The inter-facial position of this residue in both the native and mutant structures suggests that the main effect of the mutation is not the direct alteration of the size of the cavity within the core of the peptide, but the influence of neighboring residues, which leads to other structural changes in the four-α-helix scaffold (at least in the absence of halothane). Since the mutation of L38 to M38 does not alter the relative position of these residues it is possible that the structural effects of the mutation might be very different for the syn topology of $(A\alpha_2\text{–}L38M)_2$, since both L38 and L38B occupy positions within the hydrophobic core of the native syn $(A\alpha_2)_2$ peptide [22]. Further simulations are required in order to quantify this speculation.

When a single halothane molecule is placed in one of the two equivalent cavities, which exists in the core of the four-α-helix structure, features such as the components of the inertia tensor and overall degree of α-helicity are not significantly different compared to those observed for the system in the absence of halothane. This is consistent with the effect of addition of halothane to the native peptide [22]. However, upon closer examination of the mutant four-α-helix bundle

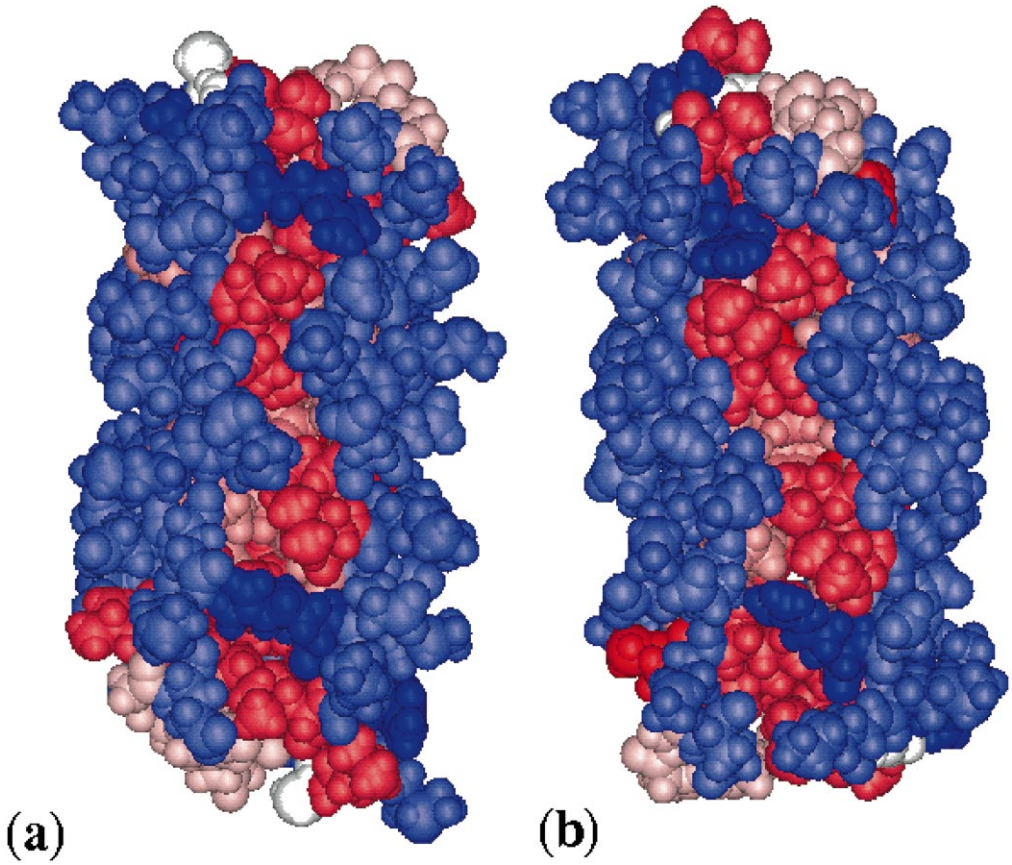

Fig. 2. Instantaneous configuration of the (a) native $(A\alpha_2)_2$ and (b) mutant $(A\alpha_2–L38M)_2$ four-α-helix bundles at 1 ns viewed from the side, illustrating the increased exposure of hydrophobic residues in the latter case. The system is colored with respect to the residue hydrophobicity. Blue corresponds to low and red to high hydrophobicity.

several interesting features are observed, which are the direct result of the presence of the anesthetic within the hydrophobic core of $(A\alpha_2–L38M)_2$.

Halothane remains within the core of the mutant $(A\alpha_2–L38M)_2$ structure during the simulation and exhibits complex translational and rotational dynamics within a single cavity. Although mobile, it occupies a position, which is consistently closer to one of the $A\alpha_2$–L38M monomers, as was observed for the native peptide [22]. The orientation of halothane in the mutant $(A\alpha_2–L38M)_2$ bundle is such that it prefers to be in a position where the C–C axis of the anesthetic molecule is parallel to the long axis of the protein, with the tri-fluorinated end towards the G loop region, and the bromine and chlorine atoms are closest to W16. No preferred orientation of the anesthetic is observed in the native $(A\alpha_2)_2$ peptide [22].

The interaction energy between halothane and a peptide residue side chain was calculated by taking the sum of the corresponding electrostatic and van der Waals components. The interaction energy between halothane and the M side chain is not significantly different as compared to the very slightly attractive interaction, which exists between the anesthetic and L38 in the native $(A\alpha_2)_2$ structure. Additionally, the location of M38 is not altered due to the presence of halothane in the simulation, i.e. it does not occupy a position within the hydrophobic core. On a single ns timescale, there is no direct contact between halothane and the mutated residue (see Fig. 3). The effect of the mutation on the protein–anesthetic interactions is likely to occur indirectly, and not as a result of the increased affinity of halothane for M rather than L.

Halothane dynamics in proximity to the mutation site in $(A\alpha_2–L38M)_2$ leads to the localized deformation of the secondary structure of one monomer in the peptide scaffold, see Fig. 4. The loss of the α-helical character of the protein in this region is illustrated by the difference in values of the torsional angles about the protein backbone between the system with and without halothane. The largest deviation from α-helicity occurs in the region of C41. Such a dramatic alteration in structure due to the presence of halothane was not observed in the native $(A\alpha_2)_2$ peptide [22]. This phenomenon appears to be the result of a combination of effects whereby the anesthetic molecule is altering specific interactions within the protein scaffold, thus causing a deformity in the α-helix close to the mutation site. For example, the interaction between halothane and C41 is significantly more attractive for the mutant $(A\alpha_2–L38M)_2$ peptide than in the native system. The loss of α-helicity in the mutant peptide in the vicinity of C41 suggests that it is this large attractive interaction between C41 and halothane, which is responsible for this structural change. However, a more complete explanation is obtained if the effect of the mutation on the overall structure of the $(A\alpha_2–L38M)_2$ peptide is included. When L38 is replaced by M38 the intra-monomer side chain packing is enhanced (for both mutant peptides with and without halothane), which in turn increases the exposure of C41 to the hydrophobic core, and hence to the anesthetic. Thus, the enhancement of interactions

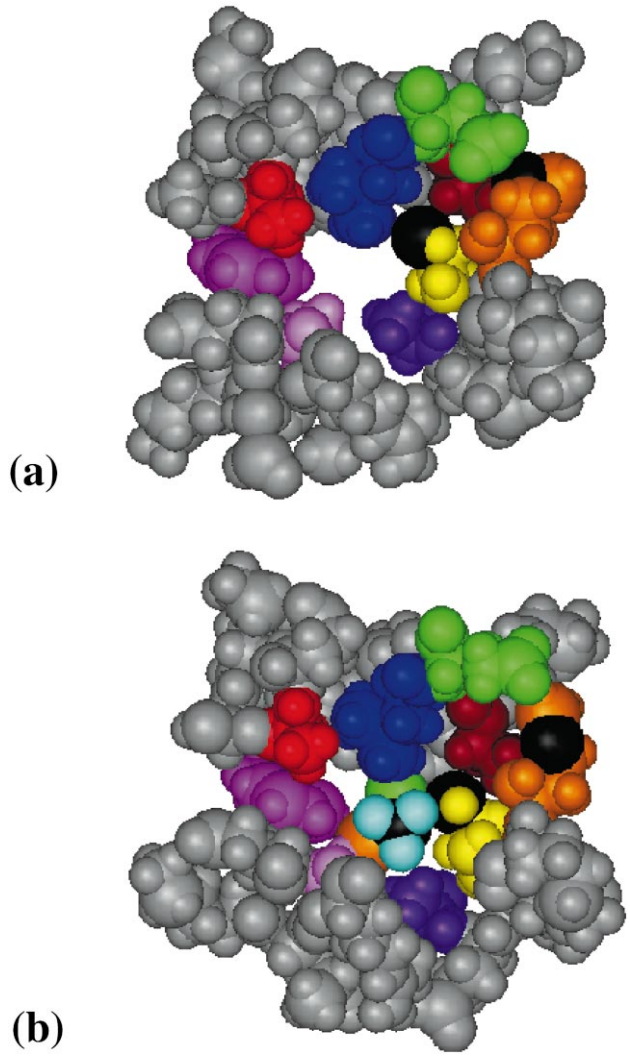

Fig. 3. Instantaneous configuration of the α-helices at 1 ns in the vicinity of the mutation site (viewed from the top) (a) in the absence and (b) in the presence of halothane. The halogen atoms in halothane are colored as: fluorine in light blue, chlorine in green and bromine in orange. Only residues associated with the hydrophobic cavity are shown. Specific residues are colored using the following code: M38 (orange), C41 (yellow), F12B (pink), L26 (dark blue), A8B (red), E27 (green), A44 (purple), A55 (pale pink), and A23 (brown). The sulphur atoms in M38 and C41 are black.

between halothane and C41 occurs as a result of the effect of the mutation on the overall structure of the four-α-helix bundle. Furthermore, this large attractive interaction between halothane and C41 can lead to a possible explanation for the preferred orientation of the anesthetic during the simulation, if the tri-fluorinated end of halothane is more attracted to the sulphur atom on C than the end of the molecule with chlorine and bromine.

The magnitudes of the average interactions between halothane and other residues within the hydrophobic cavity, such as L27 and F13B, are not significantly different compared to those observed in the native $(A\alpha_2)_2$ structure [22]. In particular, the interactions between halothane and the two W residues are only attractive for one of aromatic side chains. Furthermore, the distances between the center of mass of halothane and the center of mass of both W side chains exhibit a correlated motion. Both these observations mimic those found for the native peptide [22]. The angle between the plane of the indole rings of the two W residues and the *z*-direction has smaller fluctuations for the mutant $(A\alpha_2–L38M)_2$ structure than the native, so that in this case the W residue closest to the halothane does not alter its orientation significantly during the simulation. This apparent stability of the indole ring is probably the result of the preferred orientation of halothane in the mutant peptide, with the chlorine and bromine atoms closest to the W ring. This halothane orientation supports the experimentally observed quenching of the W fluorescence spectrum by halothane, which is the result of heavy atom interactions occurring over distances of 3–5 [32,33]. The preferred halothane orientation also decreases the fluctuations in the motion of the indole ring in the mutant $(A\alpha_2–L38M)_2$ peptide.

4. Conclusions

Several important findings have emerged from this MD simulation study. Firstly, a single halothane in the hydrophobic cavity of the mutant $(A\alpha_2–L38M)_2$ in the anti topology exhibits a preferred directionality and spatial proximity with respect to the W residues, in accordance with efficient fluorescence quenching observations [15]. Secondly, the mutated residue is not located within the hydrophobic core of this four-α-helix bundle in the anti topology, and no significant attractive interactions exist between halothane and M38. Thus, the effect of the mutation on the binding affinity of the peptide and halothane is likely an indirect one. Thirdly, the structural changes observed in the mutant bundle upon the addition of halothane are the result of a combination of the improved packing of side chains between neighboring helices on the same monomer, which increases the exposure of C41 to the hydrophobic core, and an increase in the attractive interactions between C41 and the anesthetic. Additionally, the modification to the α-helicity of the peptide scaffold due to the presence of halothane only occurs in a very localized area. Therefore, it is plausible that a second halothane molecule can be accommodated in the other, structurally equivalent hydrophobic cavity in $(A\alpha_2–L38M)_2$. The experimental stoichiometry evidence which currently exists cannot quantify the number of halothane molecules, which are bound to each peptide bundle at this level of accuracy. However, it is reasonable to assume that each four-α-helix scaffold can accommodate more than one anesthetic molecule, since the existence of halothane in one cavity does not influence the extent of the other cavity. Further simulations are required before the effects of the binding of two anesthetic molecules in the two hydrophobic cavities on the structural features of $(A\alpha_2–L38M)_2$ can be understood. The increased affinity of this mutant structure for halothane observed experimentally [15] may thus be the result of at least one halothane molecule interacting more strongly with residues such as C41 than in the native peptide, due to their deeper location in the hydrophobic core of $(A\alpha_2–L38M)_2$.

The cooperative nature of the effects, which the mutation of a single amino acid residue has on the structural and energetic features of this synthetic peptide, illustrates the subtle complexity of the interactions involved between anesthetics and proteins. The ability of computer simulation to pin-point the variation in the properties of $(A\alpha_2)_2$, as a result of a mutation

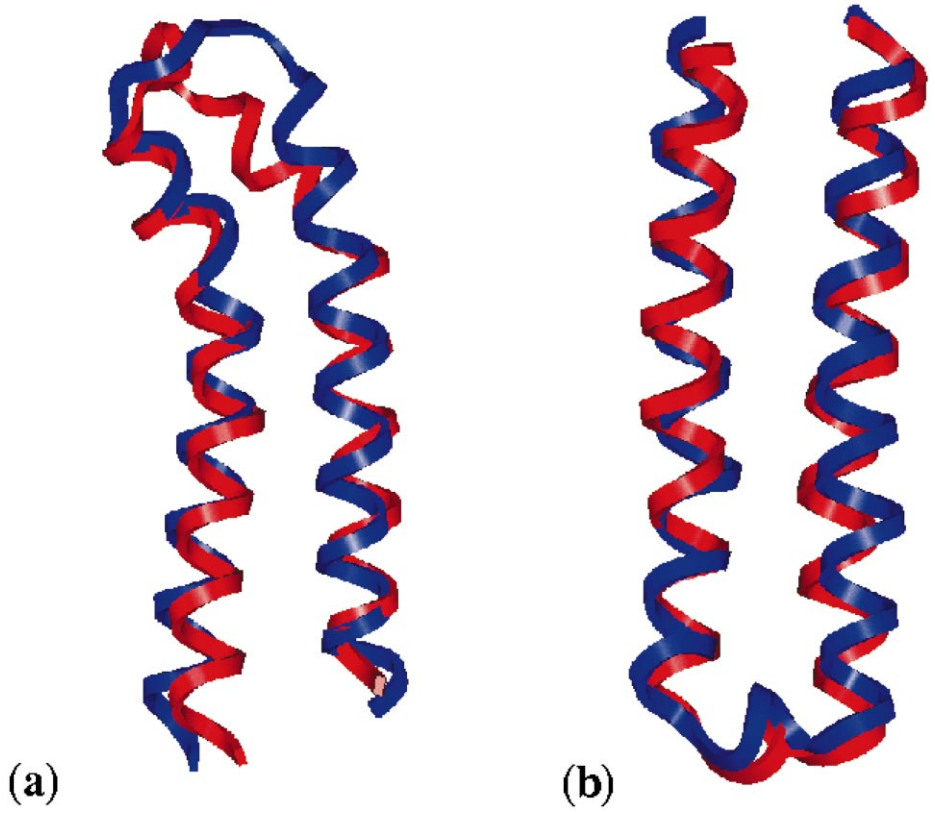

Fig. 4. Instantaneous configuration at 1 ns, of the α-helices in each of the two Aα$_2$–L38M monomers, (a) and (b), in the presence (red) and absence (blue) of halothane. The peptide backbone is shown in ribbon representation and the amino acid side chains are removed for clarity. The deformation in the α-helicity of the monomer closest to halothane is clearly illustrated.

and the addition of halothane, justifies the application of this fundamental theoretical method, and demonstrates the need to complement experiments with simulations in the study of anesthetic–protein interactions.

Acknowledgements: J.S. Johannson, P.L. Dutton, R.G. Eckenhoff, and B.R. Gibney are thanked for useful discussions, and G.J. Martyna is thanked for providing the simulation code. This research was supported by NIH grant P01 GM 55876. Computer resources were provided by the San Diego Supercomputer Center (MCA93S020) and the Pittsburgh Supercomputer Center (CHE980006P).

References

[1] Takenoshita, M. and Steinbach, J.H. (1991) J. Neurosci. 11, 1404–1412.
[2] Forman, S.A., Miller, K.W. and Yellen, G. (1995) Mol. Pharmacol. 48, 574–581.
[3] Karon, B.S., Geddis, L.M., Kutchai, H. and Thomas, D.D. (1995) Biophys. J. 68, 936–945.
[4] Eckenhoff, R.G. and Johansson, J.S. (1997) Pharmacol. Rev. 49, 343–367.
[5] Franks, N.P. and Lieb, W.R. (1994) Nature 367, 607–614.
[6] Harris, R.A., Mihic, J.C., Dildy-Mayfield, J.E. and Machu, T.K. (1995) FASEB J. 9, 1454–1462.
[7] Montal, M. (1990) FASEB J. 4, 263–265.
[8] O'Neil, K.T. and DeGrado, W.F. (1990) Science 250, 646–651.
[9] Robertson, D.E., Farid, R.S., Moser, C.C., Urbauer, J.L., Mulholland, S.E., Pidikiti, R., Lear, J.D., Wand, A.J., DeGrado, W.F. and Dutton, P.L. (1994) Nature 368, 425–432.
[10] Johansson, J.S., Rabanal, F. and Dutton, P.L. (1996) J. Pharmacol. Exp. Ther. 279, 56–61.
[11] Johansson, J.S., Gibney, B.R., Rabanal, F., Reddy, K.S. and Dutton, P.L. (1998) Biochemistry 37, 1421–1429.
[12] Rashin, A.A., Iofin, M. and Honig, B. (1986) Biochemistry 25, 3619–3625.
[13] Hubbard, S.J., Gross, K.H. and Argos, P. (1994) Protein Eng. 7, 613–626.
[14] Williams, M.A., Goodfellow, J.M. and Thornton, J.M. (1994) Protein Sci. 3, 1224–1235.
[15] Johansson, J.S., Scharf, D., Davies, L.A. and Eckenhoff, R.G. (2000) Biophys. J. 78, 982–993.
[16] Gibney, B.R., Mulholland, S.E., Rabanal, F. and Dutton, P.L. (1996) Proc. Natl. Acad. Sci. USA 93, 15041–15046.
[17] Gibney, B.R., Johansson, J.S., Rabanal, F., Skalicky, J.J., Wand, A.J. and Dutton, P.L. (1997) Biochemistry 36, 2798–2806.
[18] Gibney, B.R., Rababal, F., Skalicky, J.J., Wand, A.J. and Dutton, P.L. (1997) J. Am. Chem. Soc. 119, 2323–2324.
[19] Grosset, A.M., Rabanal, F., Farid, R.S., Robertson, D.E., Pilloud, D.L., DeGrado, W.F. and Dutton, P.L. (1996) in: Peptides: Chemistry, Structure and Biology (Kaumaya, P.T.P. and Hodges, R.S., Eds.), pp. 573–574, Mayflower Scientific Ltd., UK.
[20] Rabanal, F., DeGrado, W.F. and Dutton, P.L. (1996) J. Am. Chem. Soc. 118, 473–474.
[21] Betz, S.F., Liebmann, P.A. and DeGrado, W.F. (1997) Biochemistry 36, 2450–2458.
[22] Davies, L.A., Zhong, Q.F., Klein, M.L. and Scharf, D. (2000) Biophys. J., to appear.
[23] Brooks, B.R., Bruccoleri, R.E., Olafson, B.D., States, D.J., Swaminathan, S. and Karplus, M. (1983) J. Comp. Chem. 4, 187–217.
[24] Martyna, G.J., Tuckerman, M.E., Tobias, D.J. and Klein, M.L. (1996) Mol. Phys. 87, 1117–1157.
[25] Martyna, G.J., Samuelson, S., Hughes, A., Tobias, D.J., Yarne, D., Klein, M.L. and Tuckerman, M.E., unpublished.
[26] Darden, T., York, D. and Pedersen, L. (1993) J. Chem. Phys. 98, 10089–10092.
[27] Weiner, S.J., Kollman, P.A., Case, D.A., Singh, U.C., Ghio, C., Alagona, G., Profeta Jr., S. and Weiner, P. (1984) J. Am. Chem. Soc. 106, 765–783.

[28] Weiner, S.J., Kollman, P.A., Nguyen, D.T. and Case, D.A. (1986) J. Comp. Chem. 7, 230–235.
[29] Cornell, W.D., Cieplak, P., Bayly, C.I., Gould, I.R., Merz, K.M., Ferguson, D.M., Spellmeyer, D.C., Fox, T., Caldwell, J.W. and Kollman, P.A. (1995) J. Am. Chem. Soc. 117, 5179–5197.
[30] Jorgensen, W.L., Chandresekhar, J., Madura, J.D., Impey, R.W. and Klein, M.L. (1983) J. Chem. Phys. 79, 926–935.
[31] Scharf, D. and Laasonen, K. (1996) Chem. Phys. Lett. 258, 276–282.
[32] Tsao, D.H.H., Casa-Finet, J.R., Maki, A.H. and Chase, J.W. (1989) Biophys. J. 55, 927–936.
[33] Basu, G., Anglos, D. and Kuki, A. (1993) Biochemistry 32, 3067–3076.